Deliverable D4.3.5
Innovative design of a hybrid-type jacket for 10MW turbines

Agreement n.:	308974
Duration	November 2012 – October 2017
Co-ordinator:	DTU Wind

The research leading to these results has received funding from the European Community's Seventh Framework Programme FP7-ENERGY-2012-1-2STAGE under grant agreement No. 308974 (INNWIND.EU).

Document information

Document Name:	**Innovative design of a hybrid-type jacket for 10MW turbines**
Document Number:	**Deliverable D4.3.5**
Author:	**Jan Häfele, Cristian G. Gebhardt, Raimund Rolfes (LUH)**
Document Type	Report
Dissemination level	PU
Review:	**Daniel Kaufer**
Date:	**2016-08-31**
WP:	**4 Offshore Foundations and Support Structures**
Task:	**4.3 Structural Implementation**
Approval:	Approved by WP Leader

TABLE OF CONTENTS

1 INTRODUCTION

The cost-efficient design of offshore substructures for high-power wind energy converters is challenging. Effects like low rotor speed, high rotor thrust, and deep water levels lead to problems in ultimate limit state (ULS) or fatigue limit state (FLS) design which partly became, for instance, apparent in the design solution of the INNWIND.EU 10 MW reference jacket [1]. Additionally, some hotspots have a fatigue lifetime of 4 years, e.g. at the lowest double K-joint layer. In order to face both the cost optimization and issues concerning structural design problems of the substructure, several ideas and inventions have been developed. Some of them have been included in the innovative design of a 10 MW steel-type jacket [2]. Another promising approach to less expensive jacket designs is the hybrid jacket that incorporates steel as well as sandwich tubes. Sandwich tubes have been investigated on component level in the INNWIND.EU task 4.1 together with possible concepts for the connection of sandwich and steel tubes. This tube-to-tube connection is required to integrate sandwich tubes in a jacket as it is not possible to join them by welding. Several project reports illustrate the development of these technologies: Firstly, the state-of-the-art on component level was summarized [3]. Then, analyses with regard to axial and bending load bearing capacity, ductility behavior, plastic and elastic moment capacity, and bond behavior were conducted in numerical studies and experiments [4], [5]. Then, a validation of the component tests was performed in [6]. The outcome of the component level analyses was utilized to create a preliminary hybrid jacket design [7]. A broad study on the sensitivity of natural frequencies and a comparison to the fatigue proofs of the reference jacket was conducted in this study. However, the final results of the experiments on sandwich tubes were not available at the release of the preliminary hybrid jacket design and the dimensions of the elements were estimated.

It has to be stated that even with experimental results on component level the design solution proposed in this report shall be interpreted as an initial step towards a design for this innovative substructure concept, providing rather rough topology and dimensions than exact values for all tubes. This is due to several reasons: On the one hand, more experiments have to be performed to improve the statistical significance of the corresponding results, especially S-N curves for the determination of fatigue lifetimes. On the other hand, the design methods used in this study are usually applied to steel jackets and it has not been proven yet that they are also applicable to hybrid jackets. In addition, as a full coupled and simulation based approach is used, the computational cost is increased in comparison to a state-of-the-art design procedure.

As there is no experience with hybrid jackets and therefore not even rough dimensions (to the knowledge of the author, no similar concept does exist so far), the design problem is formulated as a mathematical design problem considering a cost function as objective and relevant design states as constraints. This is solved by a meta-heuristic optimization algorithm as already performed for steel jackets, see [8].

The report is structured as follows: The second chapter describes the hybrid jacket design approach with emphasis on general design considerations, component tests, natural frequency analysis (which was particularly discussed in the previous report), load assumptions, a cost estimation, and an introduction to the optimization algorithms that are used. The subsequent part comprises the entire results, a discussion of the technology readiness level (TRL), and a cost comparison to the INNWIND.EU 10 MW reference jacket. A conclusion and outlook are given at the end of the report.

2 HYBRID JACKET DESIGN APPROACH

2.1 Design Approach

2.1.1 Design Objectives

The aim of the hybrid jacket design is to reduce entire capital expenditure (CAPEX) by incorporating steel as well as sandwich tubes and combining them reasonably in one substructure. Of course, all proofs should be fulfilled which implies that a design lifetime of 25 years shall be reached and all utilization ratios in extreme load situations are less than 1. The 10 MW reference jacket design which revealed some fatigue issues has shown that this task is very challenging.

There are different possibilities to integrate sandwich tubes, but the most promising solution is to use them as diagonal braces while maintaining the legs as welded steel tubes (see Fig. 1). The reason for this is that the load on the braces and therefore the size of the braces is smaller compared to the legs. As sandwich elements and hybrid connections are, even after component tests, still on a quite low technology readiness level, it has been decided to do so.

However, the main problem is that no existing hybrid jacket and thereby no rough dimensions or tube measures are available for comparison. To overcome this, a structural optimization scheme is utilized to get an approximate conception of the design topology and geometry. The approach is fully coupled which implies that for each jacket design a full load analysis comprising fatigue and ultimate limit state load cases is conducted. Therefore, no equivalent (static or harmonic) loads are used in any design stage. For the entire optimization scheme it is referred to section 2.6.

2.1.2 Design Standards

If possible, the design process for the hybrid-type jacket takes the same standards and guidelines as a basis that have been used for the reference jacket design. Mainly, this is the standard IEC 61400-3 [9] which states general design requirements for offshore wind turbines. The design of the substructure bases on the offshore standard DNV OS-J101 [10] and subsequent recommended practices where particularly DNV GL 0005 [11] is of high importance for the calculation of tubular joint fatigue lifetimes. The calculation of ultimate limit state proofs is performed according to Norsok N-004 [12]. Moreover, it is common practice to calculate p-y-curves for soil-structure interaction according to API [13].

Additionally, the safety factors that have been used for the reference jacket design are adopted for the hybrid jacket design approach, see [1].

2.1.3 Software and Design Tools

The design process for offshore wind turbine substructures requires numerical time domain calculations [9]. Many tools and frameworks exist for this purpose.

The INNWIND.EU 10 MW reference jacket has been designed with several Rambøll in-house tools. These applications are proprietary which implies that the hybrid jacket design has to be obtained with other design tools. This study depends mainly on the aero-hydro-servo-elastic simulation framework FAST, developed by the National Renewable Energy Laboratory (NREL), for all time domain simulations.

With the release of the version v8, a modular structure was introduced in FAST which is illustrated in Fig. 2: Modular structure of aero-hydro-servo-elastic simulation framework FASTFig. 2. In particular, the SubDyn module enables the representation of bottom-fixed multi member

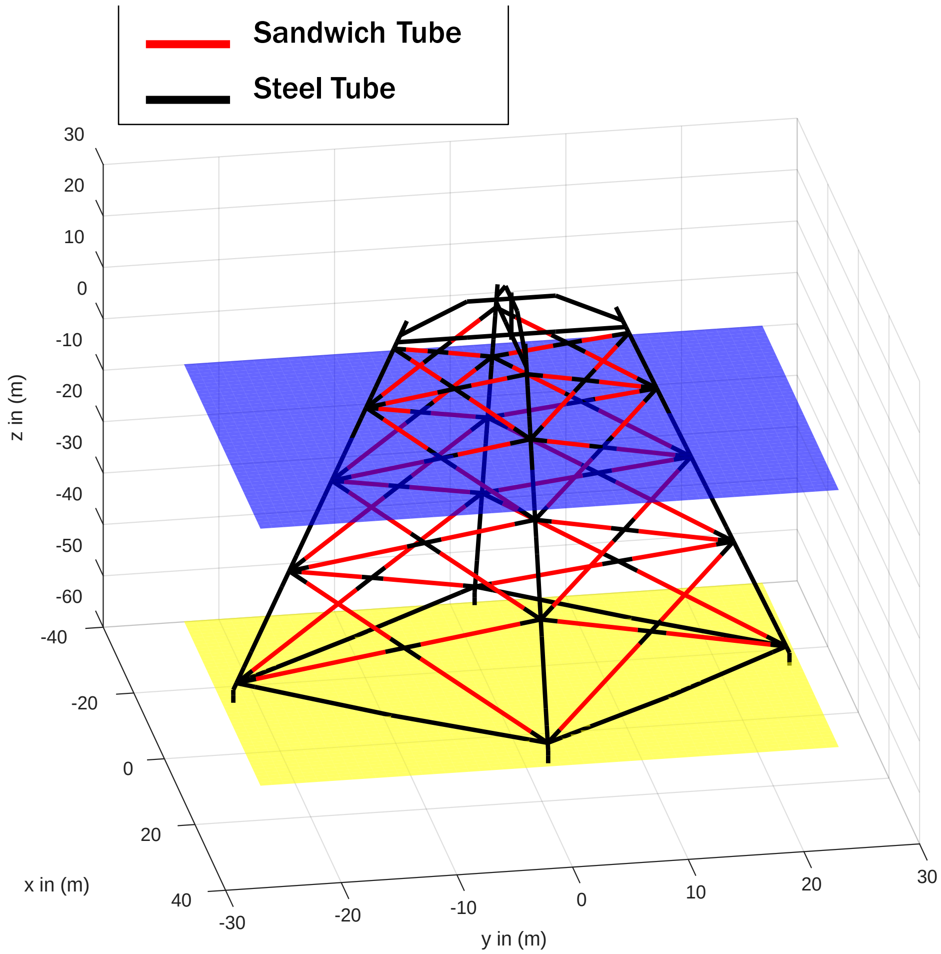

Fig. 1: INNWIND.EU 10 MW reference jacket with steel legs and sandwich braces

substructures like jackets by a finite element approach where the structure is discretized with beam elements. In order to reduce numerical expense a Craig Bampton reduction scheme was implemented [14]. Additionally, improvements have been incorporated to consider the effect of soil-structure interaction in [15] and have been extended in [16].

To generate turbulent wind fields for all design load cases, TurbSim is used. Moreover, rotor blade and tower mode shapes are computed with BModes. Pre- and postprocessing routines – implying standards for FLS and ULS proofs and all interface functions for file input and output – are implemented in MATLAB.

However, FAST is not capable to perform the calculation of eigen frequencies (this feature was available in older versions, but has not been implemented in the modularization framework yet). To overcome this drawback, the natural frequency analysis is performed with ANSYS. For both FAST and ANSYS, a structural finite element model with Timoshenko beam elements is chosen. Moreover, the same mesh sizes are used.

All time domain simulations are conducted with 780 s total simulation time from which the first 180 s are discarded due to transient decay.

FAST input files (and the Bladed-style controller DLL) for the DTU 10 MW wind turbine have been developed and published within the European project LIFES50+ [17]. As this project addresses floating substructure and a bottom-fixed substructure was not part of this project, the INNWIND.EU 10 MW reference jacket model for SubDyn has been developed during this work.

2.1.4 General Simplifications

In order to enable a hybrid jacket design in reasonable time, the problem has to be simplified. Hence, this study presumes some simplifications:

- The material properties of sandwich tubes are linearized for time domain simulations. A consideration of nonlinear structural behavior would increase the computational cost massively and is not in relation to the expected overvalue.
- Beam elements are utilized for the structural discretization in finite element models. All sandwich elements are represented by one beam element with equivalent material properties.
- In all structural analyses using beam elements, there is an overlap of non-straight connecting tubes which leads to an overestimation of mass.
- Structural meshes do not consider gaps between attached braces in double-K joints or between the lowermost double-Y joint and mud brace.
- The elastic behavior of all joints (steel and hybrid joints) is neglected.
- The pile foundation of the reference jacket is adapted without modifications.
- The hybrid jacket design does not comprise structural details like access ladders, boat landings, J-tubes, or anodes.
- The transition piece is considered as a rigid body with mass and inertia tensor rigidly connected to the uppermost nodes of the jacket (so called interface joints).
- All degradation effects impacting the structural behavior (corrosion, scour, soil degradation) are neglected, regardless of whether they are beneficial or harmful for extreme loads or fatigue lifetimes, respectively. Concerning marine growth, the assumptions that were made for the reference jacket design have been adopted (density: $1400\ \mathrm{kg/m^3}$, thickness $100\ \mathrm{mm}$ from MSL to water depth of $40\ \mathrm{m}$, thickness $50\ \mathrm{mm}$ below water depth of $40\ \mathrm{m}$).
- Linear damage accumulation is assumed for all fatigue calculations (welded and hybrid joints).
- The load case set is reduced in order to decrease the computational cost of the problem, see section 2.4.
- Non-standardized tubes are used for the preliminary design (there are actually no standardized sandwich tubes, but steel tubes) which means that tube diameters and thicknesses may change slightly for a final design approach.

2.1.5 Jacket Model

The jacket model is essential for a numerically efficient but detailed design procedure. A jacket model for steel-type jackets was proposed in [8] which is modified in the following to make it suitable for the hybrid jacket concept.

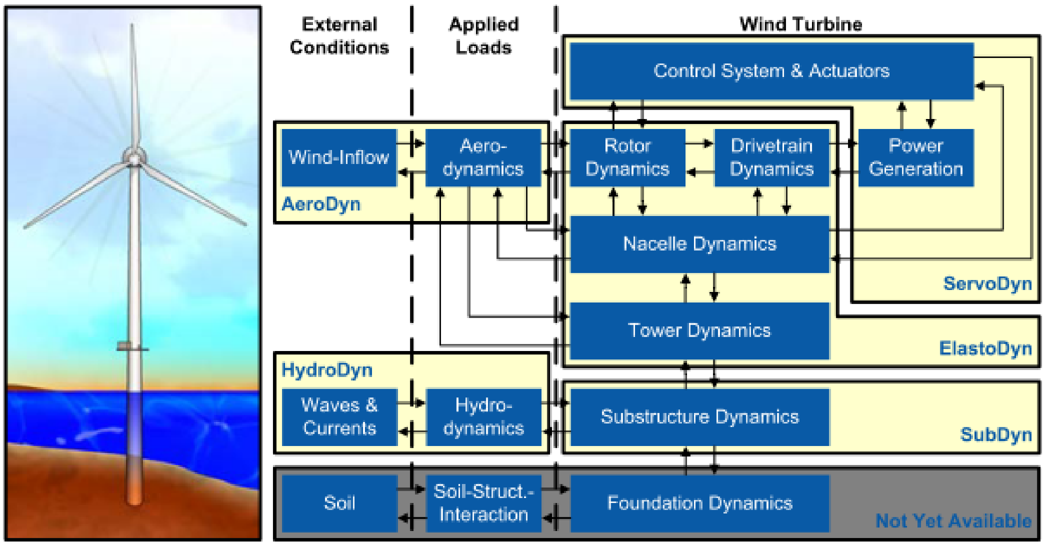

Fig. 2: Modular structure of aero-hydro-servo-elastic simulation framework FAST [18]

The jacket topology is generally defined by the number of legs N_L and the number of tiers or brace levels N_X, respectively. Each layer of nodes lies on a circle of constant height. At the lowermost (mudline) layer, the radius of this circle is R_{foot}, at the uppermost (transition piece) layer R_{head}. Both values are related by the parameter ξ:

$$\xi = \frac{R_{head}}{R_{foot}} \tag{1}$$

The distance between mudline and lowermost double K-joint layer is called L_{OSG}, the one between interface joint layer and uppermost double K-joint layer L_{TP}. Moreover, the elevation of the transition piece layer above mean sea level is L_{MSL} and with the entire jacket length L the water depth is $L - L_{MSL}$. The lowest double K-joints are connected with mud braces. A further parameter q defines the length (in z-direction) of each tier, which is simply the ratio between two consecutive tiers:

$$q = \frac{L_{i+1}}{L_i} \qquad i = 1 \dots N_X - 1 \tag{2}$$

In order to define the dimensions of steel joints, an approach is used where geometrical dimensions are defined for bottom and top layer and all intermediate values are interpolated linearly and stepwise between these boundaries. It is reasonable to utilize coupled parameters (according to [19] or [11]) for optimization to prevent getting irrational geometries, thus:

$$\beta = \frac{D_B}{D_L} \tag{3}$$

$$\gamma = \frac{D_L}{2T_L} \tag{4}$$

$$\tau = \frac{T_B}{T_L} \tag{5}$$

where D_B and D_L are the brace and leg diameter, respectively, and T_B and T_L are brace and leg thickness, respectively.

The above mentioned parameters also exist in case of a steel-type jacket. However, the different material behavior is considered by different values of Young's modulus, shear modulus and density for legs (E_L, G_L, and ρ_L) and braces (E_B, G_B, and ρ_B).

To define the sandwich tube dimensions, the parameter ω defines relations for the cross-section of a sandwich tube:

$$\omega = \frac{A_{facing} \cdot f_{y,facing}}{A_{core} \cdot f_{y,core}} \tag{6}$$

The values of $f_{y,facing}$ and $f_{y,core}$ depict the yield strengths of facing and core material, respectively. The value of ω is set to 0.3 according to common experiences with sandwich tubes [20]. Calling the measures of a sandwich tube cross section to mind (see Fig. 3), the areas A_{facing} and A_{core} can be calculated by the following equations:

$$A_{facing} = \pi \cdot ((r_4^2 - r_3^2) + (r_2^2 - r_1^2)) \tag{7}$$

$$A_{core} = \pi \cdot (r_3^2 - r_2^2) \tag{8}$$

The additional parameter ψ depicts the ratio of steel tube thickness on the one and entire sandwich tube thickness on the other side for all hybrid joints:

$$\psi = \frac{r_4 - r_1}{T_B} \tag{9}$$

This is necessary as there is no other parameter that defines the geometry of hybrid joints. The value of ψ is supposed to be 4 for the following study.

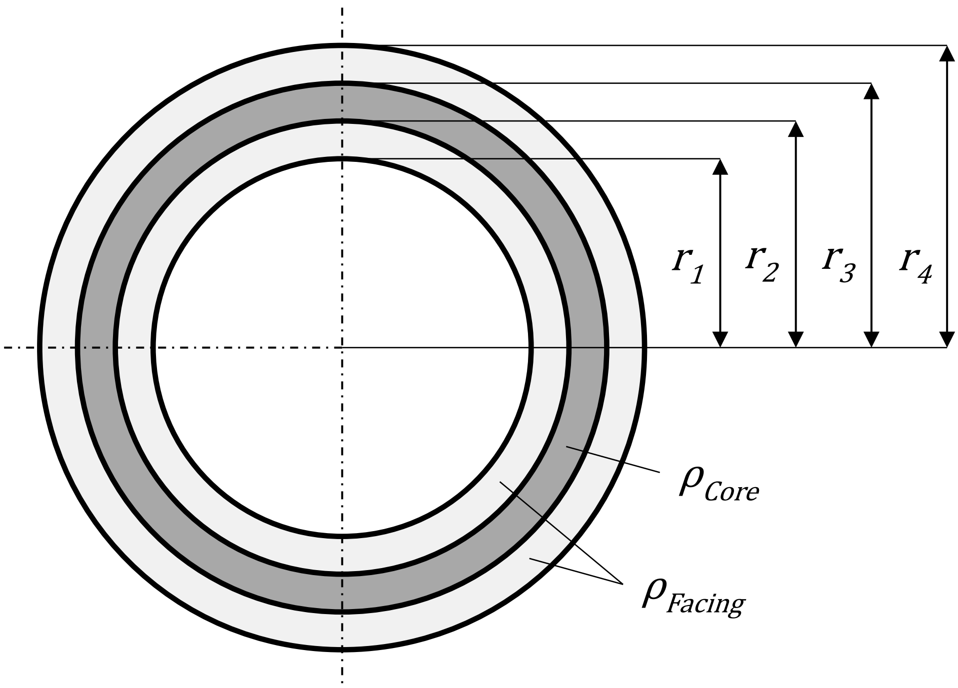

Fig. 3: Cross-section of sandwich tube with corresponding quantities

2.1.6 Design Variables

Apparently, not all parameters of the jacket model are design variables as they are determined by environmental conditions or design boundaries.

To ensure comparability to the reference jacket design concerning expenses for production infrastructure, transition piece, and transport and installation, the number of legs is fixed to a value of four. For given water depth and transition piece elevation above mean sea level, the entire jacket length is predetermined. The distances between transition piece and uppermost as well as between ground and lowermost K-joint layer are each fixed to $3\ \mathrm{m}$. Moreover, the use of steel (S355) and concrete yields the physical material properties. In this study a concrete with a density of $\rho_{Core} = 2300\ \mathrm{kg/m^3}$ is assumed and linearized in the operation point of tension. One can define a mean density of the sandwich tube $\bar{\rho}_{Sandwich}$ for each element which can be interpreted as a substitute element:

$$\bar{\rho}_{Sandwich} = \rho_B = \frac{\rho_{Core} \cdot (r_3^2 - r_2^2) + \rho_{Facing} \cdot (r_4^2 - r_3^2 + r_2^2 - r_1^2)}{r_4^2 - r_1^2} \tag{10}$$

where ρ_{Facing} is the density of the material used for the facing, thus steel with $7850.0\ \mathrm{kg/m^3}$.

All parameters of the jacket model are condensed in Table 1. Design variables can be identified by a value range, fixed parameters are denoted by a single value.

Table 1: Parameters of the jacket model with chosen parameter ranges

Parameter	Description	Value	Unit
N_L	Number of legs	4	-
N_X	Number of tiers/layers	2 ... 5	-
R_{foot}	Foot radius of jacket	10.0 ... 35.0	m
ξ	Ratio of head radius to foot radius	0.2 ... 0.8	-
L	Total jacket length	76.0	m
L_{OSG}	Length of lowest jacket members	3.0	m
L_{MSL}	Distance from TP top to water surface	26.0	m
L_{TP}	Height elevation of transition piece	3.0	m
q	Length ratio of two consecutive jacket segments	0.6 ... 1.4	-
D_L	Outer diameter of jacket legs	1.1 ... 2.5	m
β_b	Ratio of brace diameter to leg diameter at the jacket bottom	0.3 ... 0.9	-
β_t	Ratio of brace diameter to leg diameter at the jacket top	0.3 ... 0.9	-
γ_b	Ratio of leg radius to leg thickness at the jacket bottom	12.0 ... 30.0	-
γ_t	Ratio of leg radius to leg thickness at the jacket top	12.0 ... 30.0	-
τ_b	Ratio of brace thickness to leg thickness at the jacket bottom	0.3 ... 0.9	-
τ_t	Ratio of brace thickness to leg thickness at the jacket top	0.3 ... 0.9	-
ω	Ratio of facing axial force to core axial force in sandwich tubes	0.3	-
ψ	Ratio of sandwich tube to steel tube thickness in hybrid joints	4.0	-
E_L	Young's modulus of material for legs	2.1×10^{11}	$\mathrm{N/m^2}$
G_L	Shear modulus of material for legs	8.1×10^{10}	$\mathrm{N/m^2}$
ρ_L	Density of material for legs	7850.0	$\mathrm{kg/m^3}$
E_B	Young's modulus of material for braces (linearized)	2.1×10^{11}	$\mathrm{N/m^2}$
G_B	Shear modulus of material for braces (linearized)	8.1×10^{10}	$\mathrm{N/m^2}$
ρ_B	Density of material for braces (linearized)	depending on geometry	$\mathrm{kg/m^3}$
x_{MB}	Flag that determines the presence of mud braces	false/true	-

2.2 Component Tests

2.2.1 Sandwich Tube Experiments

Sandwich tubes are rod-like structural components consisting of three components: Two relatively thin steel tubes and a core made of ultra high performance concrete (UHPC). For the fabrication of hybrid tubes, two steel tubes are aligned concentrically with each other and UHPC is pumped as core material into the resulting gap. The still relatively thin core layer of ultra-high performance concrete forms the main component of the structural cross section. The main task of the core layer is to receive the compression stresses. The inner and outer steel sheets surrounding the core create a predictable amount of ductility through supporting effects. Extensive experimental investigations on the structural behaviour of these hybrid tube structures under static axial load showed that a relatively small amount of steel leads to a sufficient structural ductility [20]. Fig. 4 shows a hybrid tube test specimen under static centric loading conditions and a top view of a hybrid tube.

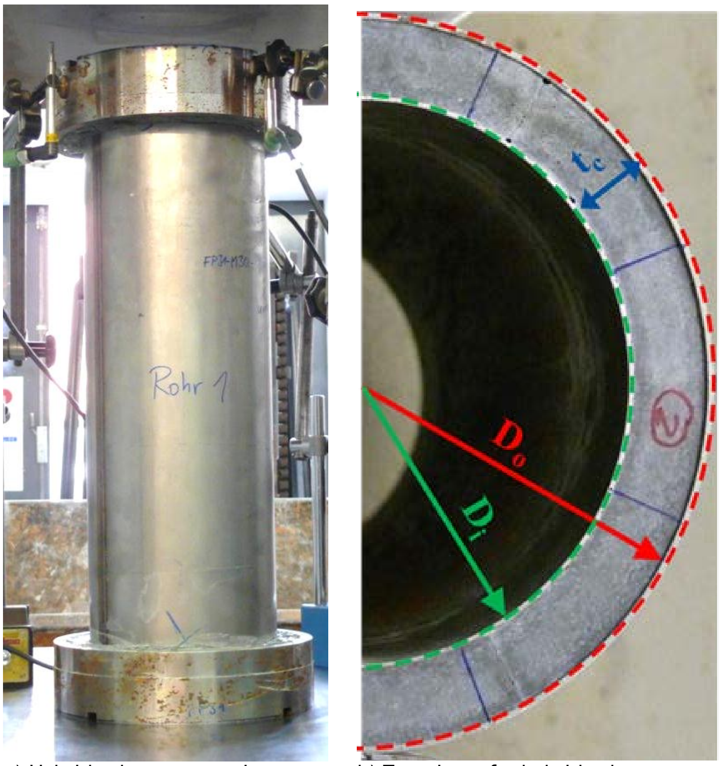

a) Hybrid tube test specimen   b) Top view of a hybrid tube

Fig. 4: Hybrid tube test specimen a) and cross section b)

The conducted experiments lead to several results with particular regard to the behavior under ultimate limit state loading conditions and some investigations of the fatigue behaviour. The entire results of sandwich tubes experiments are summarized in [21] and the reports on component level [3]–[6].

2.2.2 Hybrid Joint Experiments

The utilization of sandwich tubes requires innovative tube-to-tube connections. For this purpose, the hybrid joint concept has been introduced in work package 4.1 and described in all reports on component level. The proposed hybrid jacket concept incorporates hybrid joints to connect sandwich and steel tubes.

The scheme of a hybrid joint is shown in Fig. 5. The adhesive connection can be roughly described by the medium pipe radius r and the overlap length l. The shear stress $\tau_{nominal}$ can then be obtained by the following equation:

$$\tau_{joint} = \frac{F}{\pi \cdot r \cdot l} \tag{11}$$

where F is the force component acting axially on the joint. To address the fact that scaled specimens have been used for the component tests, a scale factor is applied. This factor was found as 3.1.

One result of the experimental tests on hybrid joints is the S-N curve shown in Fig. 6. A high scatter is obvious in these results and the coefficient of determination is quite weak with a value of 0.44 which is due to a low number of experiments and one specimen that failed very early. As a consequence, the mean regression curve and an overlap length of $0.5\ \mathrm{m}$ is used for the hybrid jacket design.

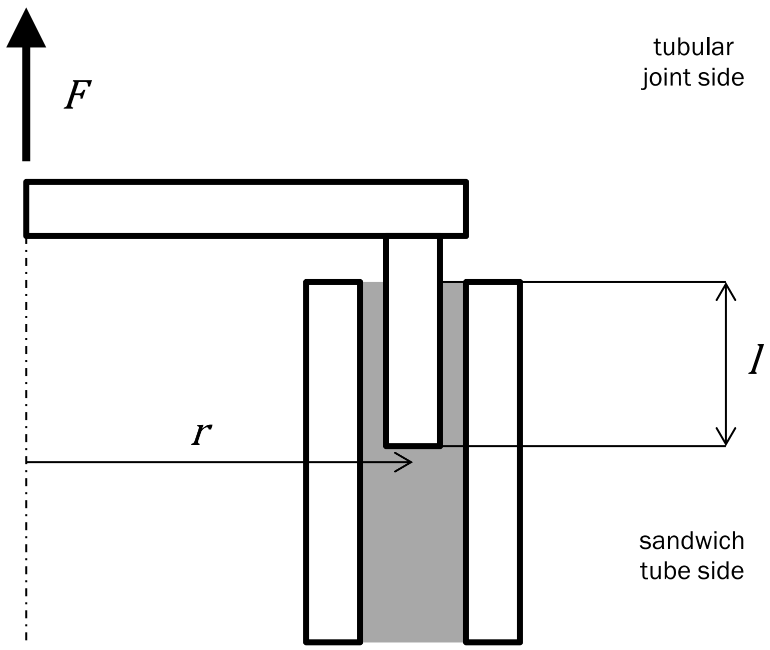

Fig. 5: Schematic illustration of the hybrid joint concept with measures used for shear stress calculation

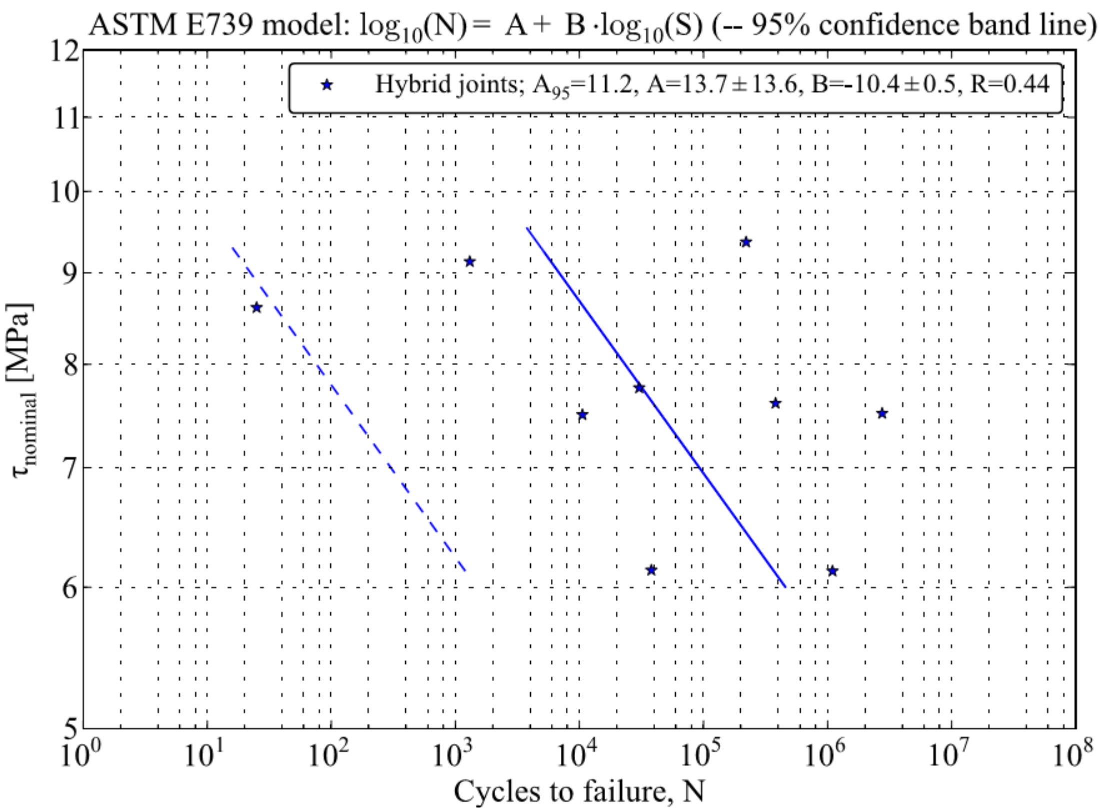

Fig. 6: Experimental S-N curve for hybrid joints

The entire results of hybrid joint experiments are summarized in the reports on component level [3]–[6].

2.3 Natural Frequency Analysis (NFA)

For a natural frequency analysis, some parameters characterizing sandwich tubes have been introduced in the preliminary hybrid jacket design report [7].

To characterize several variants of sandwich elements, two auxiliary measures and one boundary condition are defined (since there are three thicknesses, at least three equations are necessary to describe a sandwich element). The factor c_1 is defined as the proportion of the core thickness to the thickness of the corresponding thickness of the reference jacket steel tube t_{ref}:

$$c_1 = \frac{r_3 - r_2}{t_{ref}} \tag{12}$$

The factor c_2 defines the proportion of the sandwich tube thickness to the reference jacket steel tube thickness:

$$c_2 = \frac{r_4 - r_1}{t_{ref}} \tag{13}$$

Table 2: Calculated eigen frequencies (in Hz) for the entire hybrid jacket structure including tower and tower-top mass [7] (only results of hybrid jacket with sandwich braces and steel legs), relative change of hybrid jacket eigen frequencies compared to correspondent steel structure eigen frequencies (in brackets)

	1st side-side	1st fore-aft	1st torsional	2nd side-side	2nd fore-aft
Sandwich braces, steel legs $c_1 = 0,2$ $c_2 = 1,0$	0.2924 (+0.0%)	0.2944 (+0.0%)	0.9223 (+0.0%)	1.2074 (+0,4%)	1.2349 (+0,4%)
Sandwich braces, steel legs $c_1 = 0,3$ $c_2 = 1,0$	0.2924 (+0.0%)	0.2944 (+0.0%)	0.9223 (+0.0%)	1.2096 (+0.5%)	1.2375 (+0.6%)
Sandwich braces, steel legs $c_1 = 0,4$ $c_2 = 1,0$	0.2924 (+0.0%)	0.2944 (+0.0%)	0.9224 (+0.0%)	1.2117 (+0.7%)	1.2401 (+0.9%)
Sandwich braces, steel legs $c_1 = 0,3$ $c_2 = 0,8$	0.2923 (+0.0%)	0.2943 (+0.0%)	0.9162 (-0.7%)	1.2045 (+0.1%)	1.2313 (+0.1%)
Sandwich braces, steel legs $c_1 = 0,3$ $c_2 = 1,2$	0.2925 (+0.0%)	0.2945 (+0.0%)	0.9264 (+0.4%)	1.2115 (+0.7%)	1.2399 (+0.8%)

Obviously for $c_1 = 0$ and $c_2 = 1$ one gets the steel reference jacket. Moreover, it is assumed that the thicknesses of inner and outer facings are identical:

$$r_2 - r_1 = r_4 - r_3 \tag{14}$$

As mentioned above, all natural frequencies and mode shapes were calculated with ANSYS for different parameter configurations[1]. Table 2 shows that the application of sandwich braces does not affect the global natural frequencies considerably. The reason for this phenomenon is that the stiffness of the jacket structure (in a reasonable scale) is much higher than, for instance, the tower which impacts the modal behavior more significantly. This leads to the circumstance that the natural frequency analysis can be excluded from the optimization procedure in the preliminary design phase.

2.4 Load Assumptions

Commonly, a comprehensive design process for offshore structures comprises many load calculations, particularly with regard to ultimate and fatigue limit state (to cover the entire spectrum of occurring environmental conditions). For example, hundreds of computationally expensive calculations were performed to obtain one INNWIND.EU reference jacket design. Indeed, as there are no experiences with hybrid jackets and an optimization algorithm is utilized, a load case reduction is highly desirable.

2.4.1 Load Set Reduction for Fatigue Limit State (FLS)

In terms of numerical efficiency, a load set reduction, especially for FLS calculations, is highly desirable. Regarding the 10 MW reference jacket design report, one load set comprises 11 DLC 1.2 and two DLC 6.2 simulations with 2 random seeds, 12 wind directions, and 6 different wind/wave misalignments each. That results in overall 1872 time domain calculations for only one jacket design and only fatigue which is far too much for a preliminary design study. Therefore, it

[1] At this stage, the current FAST version has not the capability to compute the global eigen frequencies of the entire wind turbine. Therefore, modal analyses have been conducted in ANSYS.

has been decided to reduce the load set for each design in a reasonable way. The reduced load set is summarized in Table 3Table 2.

For this purpose, the selected wind speed bins have been regarded firstly: The load cases with 2 m/s and 30 m/s (DLC 6.4) do not play a significant role for the entire damage and were discarded from the reduced load set. This is the reason why all occurrence ratios do not add to 1. Moreover, the wind speed bins with 8 and 10 m/s, 12 and 14 m/s, and 16 and 18 m/s have each been combined which is apparently an acceptable approximation.

In addition, the effect of wind direction and wind/wave misalignment is addressed by probability distribution functions, given by the Upwind design basis [22]. As wind and wave directions are not uniformly distributed, this is a rather better approach. However, this procedure might lead to over- or underestimated loads, which is certainly weakened by increasing number of regarded load cases. Turbulent seeds for wind field (and wave) generation are chosen randomly for FLS, because it covers the real environmental behavior best.

2.4.2 Load Set Reduction for Ultimate Limit State (ULS)

The ultimate limit state load set used for the 10 MW reference jacket design report contains DLC 2.3, DLC 6.1a, and DLC 6.2a simulations. Considering all combinations of turbulent wind seeds, wind directions and wind/wave misalignments, this results again in a large number of time domain simulations.

In order to reduce the ULS load set, critical cases have been analyzed beforehand and it became apparent that always one of the load cases summarized in Table 4 is the most critical and hence decisive for the appearing extreme loads.

2.5 Cost Estimation

The initial cost model, proposed in the deliverable D1.2.3 [23], divides the capital expenses for the reference jacket in three main contributions:

- transition piece,
- jacket,
- piles.

While it is an acceptable approximation to suppose that the costs for transition piece and the piles will not change remarkably in case of a hybrid-type jacket, one has to reconsider the cost estimation for the jacket itself. However, the proposed approach only assumes a mass-dependency which is too weak for a comparison with a complete new concept. In order to predict the production costs in an appropriate way and incorporate them in the optimization procedure, one has to distinguish steel and sandwich tube costs. While the cost model provides unit costs for steel jackets (with respect to mass), there is no experience on unit costs for sandwich tubes which is far more difficult. To handle this in a simple way the costs for the hybrid jacket are separated into steel tube (4.8 €/kg, taken from the initial cost model) and sandwich tube costs (supposed to be as 7.2 €/kg, hence 50% higher[2]).

[2] The cost assumption for sandwich elements shall comprise additional expenses for material (tubes and hybrid joints) and more elaborate production complexity. However, the value is a mixed calculation as no detailed experiences on cost assessments of hybrid-type jackets are available.

Table 3: Reduced load set for fatigue limit state proofs ([1] All probability distributions of wind, wave and current directions for fatigue limit state load cases are given by the Upwind design basis [22]), design load cases according to IEC-61400-3 [9]

Load set part	1	2	3	4	5	6	7	8
DLC	1.2	1.2	1.2	1.2	1.2	1.2	1.2	1.2
Turbulent seed	random	random	random	random	random	random	random	random
Wind speed (m/s)	4.0	6.0	9.0	13.0	17.0	20.0	22.0	24.0
Wind turbulence (%)	20.4	17.5	15.6	14.4	13.8	13.4	13.3	13.1
Wind direction (°)	1)	1)	1)	1)	1)	1)	1)	1)
Water level (m)	+1.16	+1.16	0	0	+3.29	+3.29	+3.29	+3.29
Significant wave height (m)	1.10	1.18	1.31	1.48	1.70	2.76	3.09	3.42
Wave period (s)	5.88	5.76	5.70	5.96	6.50	6.99	7.40	7.80
Wave direction (°)	1)	1)	1)	1)	1)	1)	1)	1)
Near surf. curr. spd. (m/s)	0.6	0.6	0.6	0.6	0.6	0.6	0.6	0.6
Sub surf. curr. spd. (m/s)	0	0	0	0	0	0	0	0
Currrent direction (°)	0	0	0	0	0	0	0	0
Yaw error (°)	8	8	8	8	8	8	8	8
Occurrence ratio	0.109	0.124	0.281	0.251	0.141	0.042	0.036	0.016

Table 4: Reduced load set for ultimate limit state proofs, design load cases according to IEC-61400-3 [9]

Load set part	1	2	3	4	5	6	7	8
DLC	1.6	1.6	2.3	2.3	6.1	6.1	6.1	6.1
Turbulent seed	worst case	worst case	worst case	worst case	worst case	worst case	worst case	worst case
Wind speed (m/s)	12.0	12.0	12.0	12.0	42.7	42.7	42.7	42.7
Wind turbulence (%)	14.6	14.6	14.6	14.6	11.0	11.0	11.0	11.0
Wind direction (°)	0	45	0	0	0	45	0	45
Water level (m)	0	0	0	0	0	0	0	0
Significant wave height (m)	9.40	9.40	1.70	1.70	9.40	9.40	9.40	9.40
Wave period (s)	13.70	13.70	5.88	5.88	13.70	13.70	13.70	13.70
Wave direction (°)	0	45	0	0	0	45	90	135
Near surf. curr. spd. (m/s)	0.6	0.6	0.6	0.6	0.6	0.6	0.6	0.6
Sub surf. curr. spd. (m/s)	0.6	0.6	0	0	0.6	0.6	0.6	0.6
Currrent direction (°)	0	45	0	0	0	45	90	135
Yaw error (°)	8	8	8	8	8	8	8	8
Grid loss at (s)	-	-	30	30	-	-	-	-

Indeed, the cost model neglects the explicit expenses for joining tube elements and includes them in the tube unit costs. This is actually a massive simplification due to a lack of knowledge about the composition of costs for a hybrid jacket. Of course, the optimization procedure allows the incorporation of more sophisticated cost models. This point has to be addressed in further research activities.

2.6 Optimization Algorithm

Gradient-based optimization algorithms are often not suitable for the solution of the substructure design optimization problem due to the following reasons:

- It cannot be guaranteed that the optimization space is convex. Whereas, multiple local minima might occur.
- The problem can involve real and discrete (variables). Usually, gradient-based algorithms are usually not applicable to these type of problems.

With the availability of more computational capacity for lower budget, meta-heuristic optimization approaches have become a serious alternative for structural optimization problems, particularly in the last decade.

In order to obtain a cost-efficient hybrid jacket design, a Particle Swarm Optimization algorithm as proposed in [8] shall be utilized. Therefore, this section illustrates the theory and the required problem formulation.

2.6.1 Problem Formulation

It is presupposed that a jacket design is characterized by a set of design variables assembled in the vector x. For each design set, the CAPEX costs C_{total} can be evaluated, thus:

$$C_{total} = C_{total}(x) \tag{15}$$

In addition, the Boolean variables α_1 and α_2 indicate whether the jacket design fulfills all fatigue and ultimate limit state proofs, respectively. The costs are supposed to be the objective $f(x)$ of the optimization problem. To level the dimensions, the value is logarithmized:

$$f(x) = \log_{10} C_{total}(x) \tag{16}$$

The design proofs act as constraints, therefore:

$$g_1(x) = \alpha_1 \tag{17}$$

$$g_2(x) = \alpha_2 \tag{18}$$

Now, the mathematical problem formulation is stated as follows:

$$\begin{aligned} &\min f(x) \\ &\text{subject to } x_{lb} \le x \le x_{ub} \text{ and } g_i(x) = 0 \text{ for } i = 1,2 \end{aligned} \tag{19}$$

The optimization scheme is illustrated in Fig. 7. The approach is fully coupled which implies that for every set of design variables a full fatigue and extreme load set has to be calculated. This elaborate procedure requires high computation times which is discussed in more detail in the following sections.

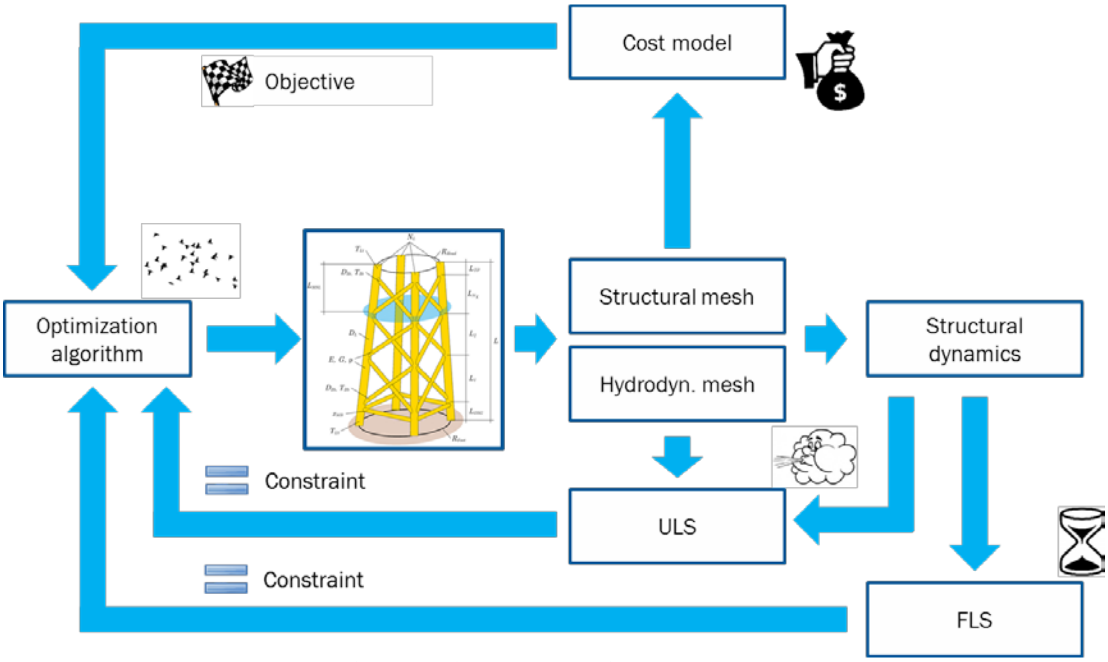

Fig. 7: Scheme of the approach for jacket optimization

2.6.2 Unconstrained Optimization Algorithm

A great deal of algorithms addressing global optimization problems are known from literature. The meta-heuristic Particle Swarm Optimization (PSO) algorithm, introduced by Kennedy and Eberhart [24], has been applied to many structural optimization problems and is outlined briefly in the following part.

The leading idea is that the social behavior of bird flocks or fish schools where each individual (also called particle) searches for the position that guarantees the best probability to get food is adopted for an unconstrained optimization algorithm:

$$\begin{aligned} &\min f(x) \\ &\text{subject to } x_{lb} \leq x \leq x_{ub} \end{aligned} \tag{20}$$

The hypothesis is that each particle – it is assumed that the position of all other J particles in the swarm is accessible for all particles – changes its own current position x_j^k depending on its own best position $x_{p,j}$ and the position of the global best particle x_g of all generations. The movement in each generation can be interpreted as velocity v_j^k that is calculated by

$$v_j^k = \omega_j^k v_j^{k-1} + c_1 r_1 \left(x_{p,j} - x_j^{k-1}\right) + c_2 r_2 \left(x_g - x_j^{k-1}\right) \tag{21}$$

In this equation, c_1 and c_2 are real constants, r_1 and r_2 are random real numbers between 0 and 1. The factor ω (introduced by Shi and Eberhart [25]) is called inertia weight. This modification of the velocity term is widely accepted in literature.

Subsequent particle positions are calculated by adding the velocity to the previous position in generation k:

$$x_j = x_j^{k-1} + v_j \tag{22}$$

The objective function is evaluated with this design variable vector and then it is decided whether this is better (better means smaller objective value in the case of minimization) than all positions the particle was in before. If so, the local best position of the corresponding particle is replaced by the current one and the next decision is made whether this position is also the global best position compared to all positions the swarm has ever reached. If so, the global best position must be updated, too.

2.6.3 Constrained Optimization Algorithm

To solve constrained problems, the ALPSO (Augmented Lagrangian Particle Swarm Optimization) approach by Sedlaczek and Eberhard [26] is used as it was found to be numerical efficient while converging well.

Firstly, a modified Lagrangian function $\mathcal{L}(x)$ is defined:

$$\mathcal{L}(x) = f(x) + \sum_{i=1}^{m_e} \lambda_i g_i(x) + \sum_{i=1}^{m_e} r_{p,i} g_i^2(x) \tag{23}$$

with the number of equality constraints m_e.

The algorithm utilizes unconstrained PSO to minimize $\mathcal{L}(x)$ instead of $f(x)$, the constrained problem is hence transformed into an unconstrained problem. After each run of unconstrained PSO, λ_i and $r_{p,i}$ are updated according to:

$$\lambda_i^{t+1} = \lambda_i^t + 2r_{p,i}^t g_i(x) \tag{24}$$

$$r_{p,i}^{t+1} = \begin{cases} 2r_{p,i}^t, & \text{if } \left|g_i\left(x_g^t\right)\right| > \left|g_i\left(x_g^{t-1}\right)\right| \wedge \left|g_i\left(x_g^t\right)\right| > \epsilon \\ \frac{1}{2}r_{p,i}^t, & \left|g_i\left(x_g^t\right)\right| \leq \epsilon \\ r_{p,i}^t, & \text{else} \end{cases} \tag{25}$$

The factor ϵ is a tolerance boundary that shall lead to better performance.

The algorithm leads to a procedure with nested loops that can be parallelized in different ways. It is therefore very suitable for numerically efficient computations.

2.6.4 Optimization Algorithm Parameters

As mentioned in the previous section, the optimization has been implemented in a way that several particles can be calculated in parallel. For this purpose, the population size has to be an integer multiple of the number of cores (here: 8). The parameters used for the computation of the ideal hybrid jacket design are summarized in Table 5.

The time needed to compute the optimization problem is the product of population size, max. inner loops, max. outer loops and the mean simulation time for all design load cases. Therefore, quite low values have been chosen for the optimization algorithm parameters to limit the entire time to obtain a solution.

Table 5: Optimization algorithm parameters

Parameter	Value
Population size	$32\ (8\ \times\ 4)$
Max. inner loops	3
Max. outer loops	10
c_1	$0{,}5$
c_2	0.5
ω	0.5
λ^0	0
r_p^0	1
ϵ	10^{-2}

3 RESULTS

3.1 Hybrid-Type Jacket Design Solution

The optimization procedure has been utilized to obtain a hybrid jacket design which is described in detail in the following sections.

3.1.1 Optimization Process and Numerical Efficiency

The entire computation of the optimization problem took approximately 53 days on an Intel Xeon E5-2687W v3 CPU with 8 cores used in parallel and 64 GB random access memory.

The global best objective value of $f(x) = 6.942$ was reached after ten outer loop generations. The jacket fulfils all fatigue and ultimate limit state proofs.

3.1.2 Topology and Geometry

The space of all possible design solutions was limited to four-legged jackets in order to make the solution comparable to the reference design. The parameters of the best solution are summarized in Table 6 (see appendix chapter A.2 for a general representation of the jacket parameters).

Compared to the reference design, the hybrid-type approach gets along with three tiers and a mud brace. The foot radius of $R\_foot = 20.34\ \mathrm{m}$ is equal to a foot print of $28.77\ \mathrm{m}$ as the jacket has four legs. Obviously, the coupled parameters have lower values at the jacket bottom meaning that the tube dimensions are bigger at the jacket top due to fatigue lifetimes (this is discussed in the following subsection): β varies from 0.72 (bottom) to 0.76 (top), γ from 16.66 (bottom) to 18.42 (top), and τ from 0.52 (bottom) to 0.56 (top). The leg diameter has a value of $1.48\ \mathrm{m}$ which is slightly more than the value of the reference jacket. Moreover, it is noticeable that parameter ξ hits the upper boundary of 0.8 (due to the cost model high values of ξ do not impact the jacket costs significantly) and q has nearly a value of 1 which means that the segment lengths of all three tiers are quite equal. All other parameters of the jacket model were not considered as design variables.

3.1.3 Fatigue Limit State Results

The most fatigue critical locations of the jacket are the hybrid joints. The proposed jacket fails after 31.27 years at joint 35 (see appendix chapter A.1) which is a X-joint in the uppermost tier. This is slightly above the design lifetime of 27 years (including 2 years additional lifetime for fatigue induced by installation and decommissioning and a damage fatigue factor of 3). The mean lifetime of all joints in the jacket is 77.35 years (standard deviation: 28.31 years) shows that the optimization approach leads to a balanced structure design.

For detailed fatigue limit state results it is referred to appendix chapter A.2.

3.1.4 Ultimate Limit State Results

The structural design is driven by fatigue lifetimes, thus all ultimate limit state utilization ratios for tubes and joints are far below 1. The most critical design load case concerning ULS is DLC 1.6 with 0° wind, wave and current direction (load set part 1, see Table 4) with utilization ratios of 0.51 for joint punching shear check and 0.59 for local tube buckling.

Table 6: Ideal jacket parameters obtained by optimization (design variables in bold)

Parameter	Description	Value	Unit
N_L	Number of legs	4	-
$\boldsymbol{N_X}$	**Number of tiers/layers**	**3**	-
$\boldsymbol{R_{foot}}$	**Foot radius of jacket**	**20.34**	m
$\boldsymbol{\xi}$	**Ratio of head radius to foot radius**	**0.8**	-
L	Total jacket length	76.0	m
L_{OSG}	Length of lowest jacket members	3.0	m
L_{MSL}	Distance from TP top to water surface	26.0	m
L_{TP}	Height elevation of transition piece	3.0	m
$\boldsymbol{q}$	**Length ratio of two consecutive jacket segments**	**1.02**	-
$\boldsymbol{D_L}$	**Outer diameter of jacket legs**	**1.48**	m
$\boldsymbol{\beta_b}$	**Ratio of brace diameter to leg diameter at the jacket bottom**	**0.72**	-
$\boldsymbol{\beta_t}$	**Ratio of brace diameter to leg diameter at the jacket top**	**0.76**	-
$\boldsymbol{\gamma_b}$	**Ratio of leg radius to leg thickness at the jacket bottom**	**16.66**	-
$\boldsymbol{\gamma_t}$	**Ratio of leg radius to leg thickness at the jacket top**	**18.42**	-
$\boldsymbol{\tau_b}$	**Ratio of brace thickness to leg thickness at the jacket bottom**	**0.52**	-
$\boldsymbol{\tau_t}$	**Ratio of brace thickness to leg thickness at the jacket top**	**0.58**	-
ω	Ratio of facing axial force to core axial force in sandwich tubes	0.3	-
ψ	Ratio of sandwich tube to steel tube thickness in hybrid joints	4.0	-
E_L	Young's modulus of material for legs	2.1×10^{11}	N/m^2
G_L	Shear modulus of material for legs	8.1×10^{10}	N/m^2
ρ_L	Density of material for legs	7850.0	kg/m^3
E_B	Young's modulus of material for braces (linearized)	2.1×10^{11}	N/m^2
G_B	Shear modulus of material for braces (linearized)	8.1×10^{10}	N/m^2
ρ_B	Density of material for braces (linearized)	depending on geometry	kg/m^3
x_{MB}	Flag that determines the presence of mud braces	false	-

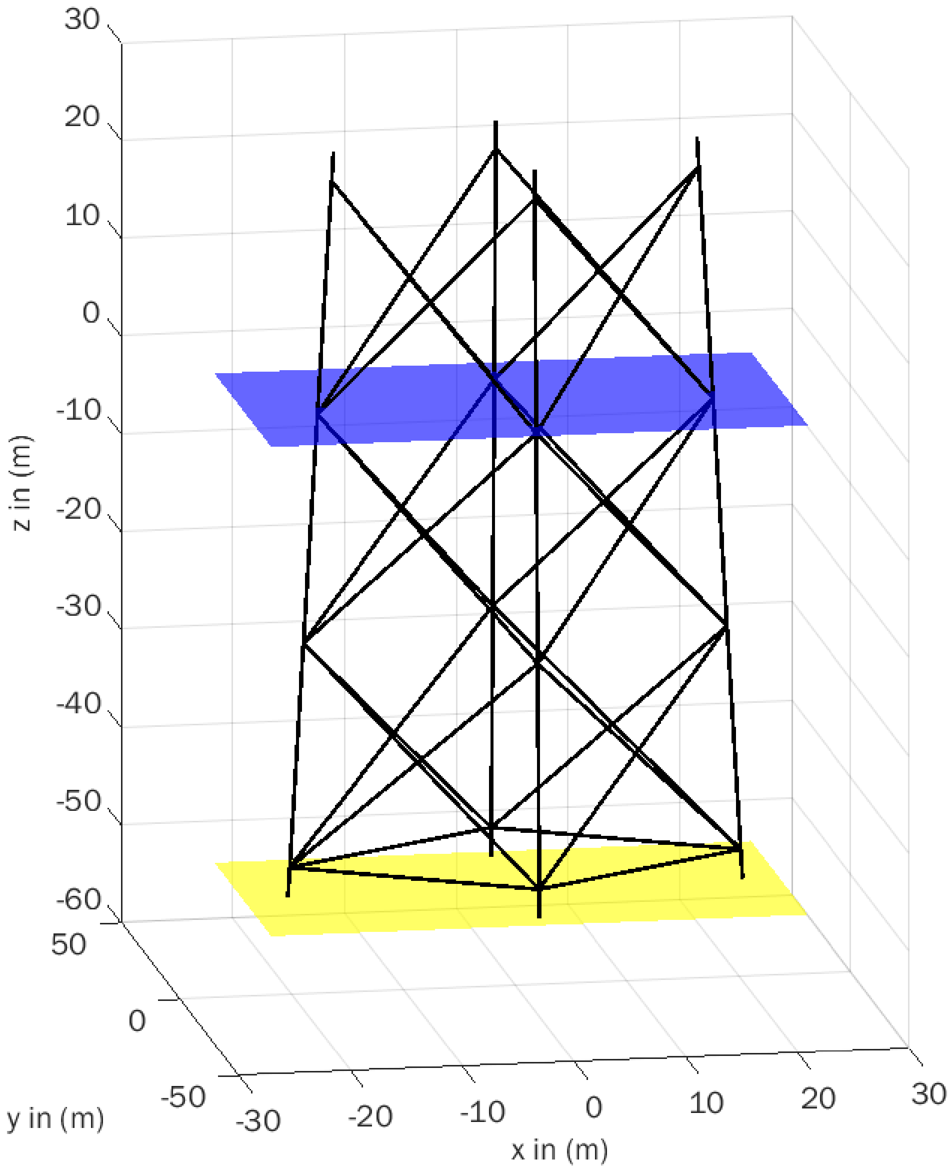

Fig. 8: Topology of ideal hybrid-type jacket design obtained by optimization approach (blue: mean sea level layer, yellow: soil layer)

3.2 Technology Readiness Level (TRL)

The hybrid jacket concept is a structure obtained by out-of-the-box-thinking that has Technology Readiness Level 2. This implies that basic principles are observed and the technology concept is formulated. In order to reach a higher TRL, experimental proofs of the concept are necessary which have only been performed for sandwich tubes and hybrid joints, but not the entire structure. Additionally, the number of component tests has to be increased in order to get more confidence of material properties.

3.3 Cost Comparison to INNWIND.EU Reference Jacket

The resulting costs of the jacket optimization procedure are shown in Table 7. The hybrid-type jacket design is a bit more expensive than the reference design (12,6 % for the jacket itself and 9.6 % for the entire structure, costs for piles and transition piece are equal) due to the higher costs of sandwich tubes, but fulfils all design proofs. The mass of the entire hybrid jacket is about 1073 tons (reference jacket: 1210 tons) whereby the steel mass is 449 tons and the concrete mass is 624 tons. Although the structure is – presuming the specified cost assumptions – more expensive, the transport and installation process can benefit from the expected lower mass of the hybrid-type jacket.

However, it has to be stated that the cost model bases on assumptions with limited significance, as the costs are only mass-dependent in this approach. Beside other aspects, this is discussed in the following section.

3.4 Benefits and Limits of the Approach, Improvement Potential

The methodology is very promising concerning the improvement potential compared to state-of-the-art jacket design approaches. The entire procedure does not require any manual design iterations of the designer and it can be supposed that the output is a jacket design that states the ideal solution with regard to costs and occurring loads.

However, some limitations have become apparent during the design procedure that are discussed in the following.

Imprecise cost model

The results show that the hybrid-type jacket is a bit more expensive than the reference jacket. Although the costs are imaginable, this value is not exact because the real cost assessment is far more sophisticated. The fabrication experiences from the experiments cannot be considered to define a more detailed cost model. These parts are prototypes and are not valid for a comparison to mass produced steel tubes. The main drawback of the cost model that has been used for this study is that it only depends on the mass of the jacket. However, expenses for joining tube elements are neglected, for instance. Therefore, the approach can be improved by a more detailed cost model if it is possible to divide the costs into more portions.

Simplified load assumptions

In order to reduce the numerical cost of the optimization procedure, the number of design load cases per load set has been decreased massively. However, these load sets are likely to depict a less conservative excitation of the structure compared to a full load set which may result in a cheaper jacket. However, considering all wind directions and wind/wave misalignments was not a meaningful option for this study where numerous different jacket design topologies and geometries have been analyzed. Nevertheless, for higher TRL levels the final design should consider a comprehensive load set.

Natural frequency analysis

The calculation of global eigen frequencies was neglected in the optimization procedure because a preliminary study (already shown in Deliverable D4.3.2 [7]) demonstrated that the utilization of sandwich elements in a jacket structure does not affect the modal behavior significantly. However, it can be supposed that the impact on local eigen frequencies (regarding the local brace motion) is more distinct. This effect has not been regarded in detail, but might be part of further studies.

Table 7: Costs and masses of steel- and hybrid-type jacket broken down to structural parts

Structural part		Reference jacket	Hybrid jacket	Difference
Piles	Mass	380 000 kg	380 000 kg	-
	Cost	456 000 €	456 000 €	-
Jacket	Mass	1 210 000 kg	1 072 740 kg	- 11.3 %
	Cost	5 808 000 €	6 646 107 €	+ 12.6 %
Transition piece	Mass	330 000 kg	330 000 kg	-
	Cost	1 650 000 €	1 650 000 €	-
Total	Mass	**1 920 000 kg**	**1 782 740 kg**	**- 7.1 %**
	Cost	**7 914 000 €**	**8 752 107 €**	**+ 9.6 %**

Experimental basis

Some experiments on scaled specimens for sandwich tubes and hybrid joints were used for the hybrid jacket design. However, in order to improve the reliability of the results, more experiments have to be performed in the future. Additionally, the scale of the specimens has to be increased to strengthen the significance of the study.

Time domain simulation

All jackets have been calculated with a FE code using linear Timoshenko beam theory though the material behavior of the regarded hybrid materials is significantly nonlinear (in particular, the nonlinear structural behavior appears in case of extreme loads). This was done because the incorporation of nonlinearities bears no relation to the estimated numerical cost that goes along with it. However, the development of advanced simulation methods for hybrid jackets have to address this aspect specially.

Optimization procedure

Regarding the preferences of the optimization algorithm in Table 5, it is obvious that both the values of population size and maximum loops are quite low in order to calculate the problem in an adequate amount of time. However, a slight improvement of the results is imaginable in case of higher population size or termination in later inner or outer loop generations.Table 5: Optimization algorithm parameters

4 CONCLUSION AND OUTLOOK

Hybrid-type jackets consist of steel and sandwich tubes and depict either an opportunity to reduce costs of substructures for offshore wind turbines or an alternative to address fatigue problems. The structural behavior of sandwich tubes and hybrid joints has been analyzed in several experiments on component level. Goal of this work was the incorporation of these innovative elements in an entire structure.

With regard to a cost reduction compared to the reference jacket design, an optimization scheme has been utilized which has been proven itself as a promising approach for ideal structure design (see [8]). Different from the reference design, several presumptions and simplifications have been made to enable a solution in a reasonable amount of time where two of them are of main importance: Firstly, a load set reduction has been proposed which covers the main loads but reduces the numerical cost considerably. Secondly, the material behavior was linearized prior to time domain simulations. However, an entire optimization procedure took almost two months of computation time with eight cores calculating in parallel.

To enable comparability to the reference jacket, the number of jacket legs was fixed to a value of four. All other design-driving parameters were considered as variable. With these boundaries, the ideal hybrid jacket design has only three tiers, but compared to the reference jacket slightly higher tube dimensions. Moreover, the resulting costs obtained by the proposed cost model are marginally higher, but in a reasonable margin and the mass of structure is lower, probably resulting in reduced transport and installation expenses.

The obtained structure should come across as an initial guess to a real structure because it depends on a rather precarious experimental basis and several simplifications during the design process that have been discussed in detail. To improve the hybrid-jacket design and thus bring it to higher Technology Readiness Level, the following questions should be addressed in further studies:

- Is the structural design affected significantly when more extensive results from experiments or better cost models are available?
- How can nonlinearities of sandwich tubes and hybrid joints be considered in time domain simulations with high demand on numerical efficiency?
- How does a concept for the industrial production of hybrid-type jackets look like? Are there elements in a supply chain of steel jackets that can be adapted? How to avoid imperfections and what are acceptable fabrication tolerances.
- What are the particular challenges on transport, installation, and decommissioning? Does the concept require special monitoring concepts?

5 REFERENCES

[1] T. von Borstel, "Design Report Reference Jacket," INNWIND.EU Deliverable D4.3.1, 2013.

[2] M. Stolpe, W. N. Wandji, A. Natarajan, R. Shirzadeh, M. Kühn, and D. Kaufer, "Innovative design of a 10MW steel-type jacket," INNWIND.EU Deliverable D4.3.4, 2016.

[3] B. Kuhnle, "State of the art on component level," INNWIND.EU Deliverable D4.1.1, 2013.

[4] N. Scholle, L. Radulović, T. Westphal, L. B. Ibsen, M. Kohlmeier, V. Fedorov, M. Sanz, J. Pöllmann, B. Kuhnle, P. Brosche, and T. von Borstel, "Innovations on component level (interim report)," INNWIND.EU Deliverable D4.1.2, 2014.

[5] N. Scholle, L. Radulović, R. Nijssen, L. B. Ibsen, M. Kohlmeier, A. Foglia, A. Natarajan, J. Thiel, B. Kuhnle, M. Kraft, M. Kühn, P. Brosche, and D. Kaufer, "Innovations on component level (final report)," INNWIND.EU Deliverable D4.1.3, 2015.

[6] N. Scholle, L. Radulović, R. Nijssen, F. Lahuerta, L. B. Ibsen, M. Kohlmeier, and A. Foglia, "Validation of innovations by tests on component level," INNWIND.EU Deliverable D4.1.4, 2015.

[7] B. Kuhnle, M. Stolpe, A. Natarajan, T. Hanis, J. Häfele, T. von Borstel, and S. Prior, "Innovative Concepts for Bottom-Mounted Structures," INNWIND.EU Deliverable D4.3.2 Revision 2, 2015.

[8] J. Häfele and R. Rolfes, "Approaching the ideal design of jacket substructures for offshore wind turbines with a Particle Swarm Optimization algorithm," in *Proceedings of the Twenty-sixth (2016) International Offshore and Polar Engineering Conference*, Rhodes, Greece, 2016.

[9] International Electrotechnical Commision, "Wind turbines – Part 3: Design requirements for offshore wind turbines," Norm IEC-61400-3:2009, EN 61400-3:2009, 2009.

[10] Det Norske Veritas AS, "Design of Offshore Wind Turbine Structures," Offshore Standard DNV-OS-J101, 2014.

[11] DNV GL AS, "Fatigue design of offshore steel structures," Recommended Practice DNVGL-RP-0005:2014-06, 2014.

[12] NORSOK, "Design of steel structures," Standard N-004 Rev. 2, 2004.

[13] API, "Recommended Practice for Planning Designing and Constructing Fixed Offshore Platforms - Working Stress Design," American Petroleum Institute, Dallas, USA, RP 2A-WSD, Dezember 2000.

[14] H. Song, R. Damiani, A. Robertson, and J. Jonkman, "A New Structural-Dynamics Module for Offshore Multimember Substructures within the Wind Turbine Computer-Aided Engineering Tool FAST," in *International Ocean, Offshore and Polar Engineering Conference*, Anchorage, AK, 2013, vol. 23.

[15] J. Häfele, C. Hübler, C. G. Gebhardt, and R. Rolfes, "An improved two-step soil-structure interaction modeling method for dynamical analyses of offshore wind turbines," *Appl. Ocean Res.*, vol. 55, pp. 141–150, 2016.

[16] C. Hübler, J. Häfele, A. Ehrmann, and R. Rolfes, "Effective consideration of soil characteristics in time domain simulations of bottom fixed offshore wind turbines," in *Proceedings of the Twenty-sixth (2016) International Offshore and Polar Engineering Conference*, Rhodes, Greece, 2016.

[17] M. Borg, M. Mirzaei, and A. Bredmose, "Wind turbine models for the design," LIFES50+ Deliverable D1.2, 2015.

[18] B. Jonkman and J. M. Jonkman, "Guide to Changes in FAST v8," National Renewable Energy Laboratory, Golden, CO, Manual, 2015.

[19] Germanischer Lloyd, “Guideline for the Certification of Offshore Wind Turbines,” Offshore Standard, 2012.

[20] N. Lindschulte, “Drucktragverhalten von Rohren aus Ultrahochfestem Beton mit Stahlblechummantelung,” Dissertation, Leibniz Universität Hannover, 2013.

[21] N. Scholle and L. Lohaus, “UHPC-Steel Hybrid Tube Components for Application in Offshore Support Structures,” in *Proceedings of the Twenty-sixth (2016) International Offshore and Polar Engineering Conference*, Rhodes, Greece, 2016.

[22] T. Fischer, W. de Vries, and B. Schmidt, “Upwind Design Basis,” 2010.

[23] P. K. Chaviaropoulos, I. Karga, C. Harkness, and B. Hendriks, “PI-based assessment of innovative concepts (methodology),” INNWIND.EU Deliverable D1.2.3, 2014.

[24] J. Kennedy and R. Eberhart, “Particle Swarm Optimization,” in *Proceedings of IEEE International Conference on Neural Networks IV*, Perth, 1995, pp. 1942–1948.

[25] Y. Shi and R. Eberhart, “A modified particle swarm optimizer,” in *The 1998 IEEE International Conference on Evolutionary Computation Proceedings*, Anchorage, AK, 1998, pp. 69–73.

[26] K. Sedlaczek and P. Eberhard, “Using augmented Lagrangian particle swarm optimization for constrained problems in engineering,” *Struct. Multidiscip. Optim.*, vol. 32, no. 4, pp. 277–286, Oct. 2006.

A. APPENDIX

A.1. HYBRID JACKET JOINT NUMBERING

By way of illustration, Fig. 9 shows the topology of the hybrid-type jacket with all joint numbers.

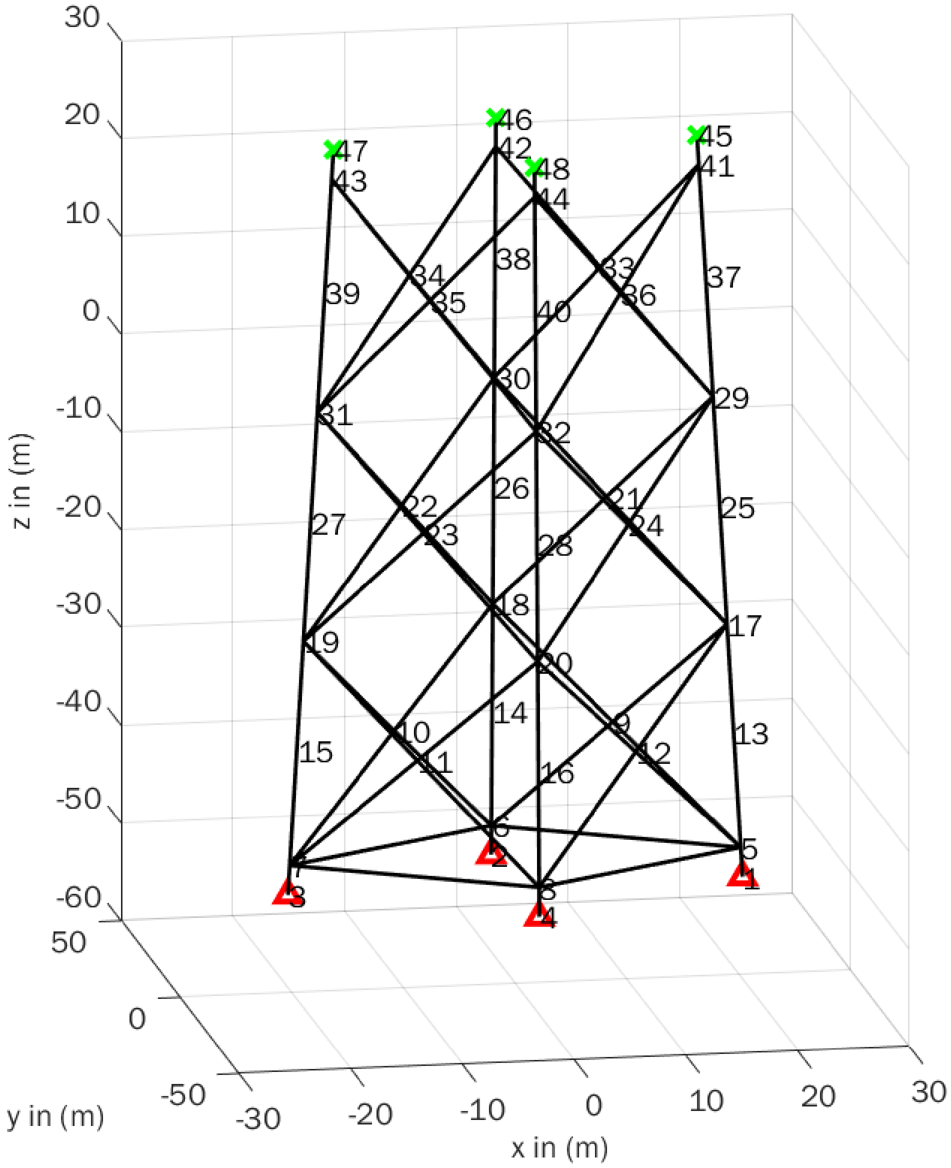

Fig. 9: Topology of ideal jacket with joint numbers (red triangles depict base joints, green crosses depict interface joints)

A.2. OVERVIEW OF HYBRID JACKET GEOMETRY AND MASS

In the style of the reference jacket design report [1] Table 8 shows the main parameters of the ideal hybrid jacket.

Table 8: Overview of Hybrid Jacket Geometry and Mass

Structural property	Value	Unit
Number of legs	4	-
Base width (foot print)	28.77	m
Top width (head print)	23.01	m
Batter angle of the legs	3	°
Jacket legs diameter (outer)	1480	mm
Jacket legs minimum wall thickness	44	mm
Jacket legs minimum wall thickness	40	mm
Number of tiers/layers	3	-
Upper tier sandwich braces diameters (outer)	1125	mm
Upper tier sandwich braces wall thickness	93	mm
Middle tier sandwich braces diameters (outer)	1095	mm
Middle tier sandwich braces wall thickness	93	mm
Lower tier sandwich braces diameters (outer)	1067	mm
Lower tier sandwich braces wall thickness	92	mm
Sandwich mud braces diameters (outer)	1067	mm
Sandwich mud braces wall thickness	92	mm
Jacket mass (including TP and foundation)	1783	tons
Jacket mass (without TP and foundation)	1073	tons
Steel mass (only jacket)	449	tons
Concrete mass (only jacket)	624	tons

A.3. FATIGUE LIMIT STATE RESULTS

Fig. 10 shows the fatigue limit state results for the ideal jacket design which comprise the ranges, minimum and maximum, and mean lifetimes of hybrid joints (tube-to-tube connections) for each joint layer.

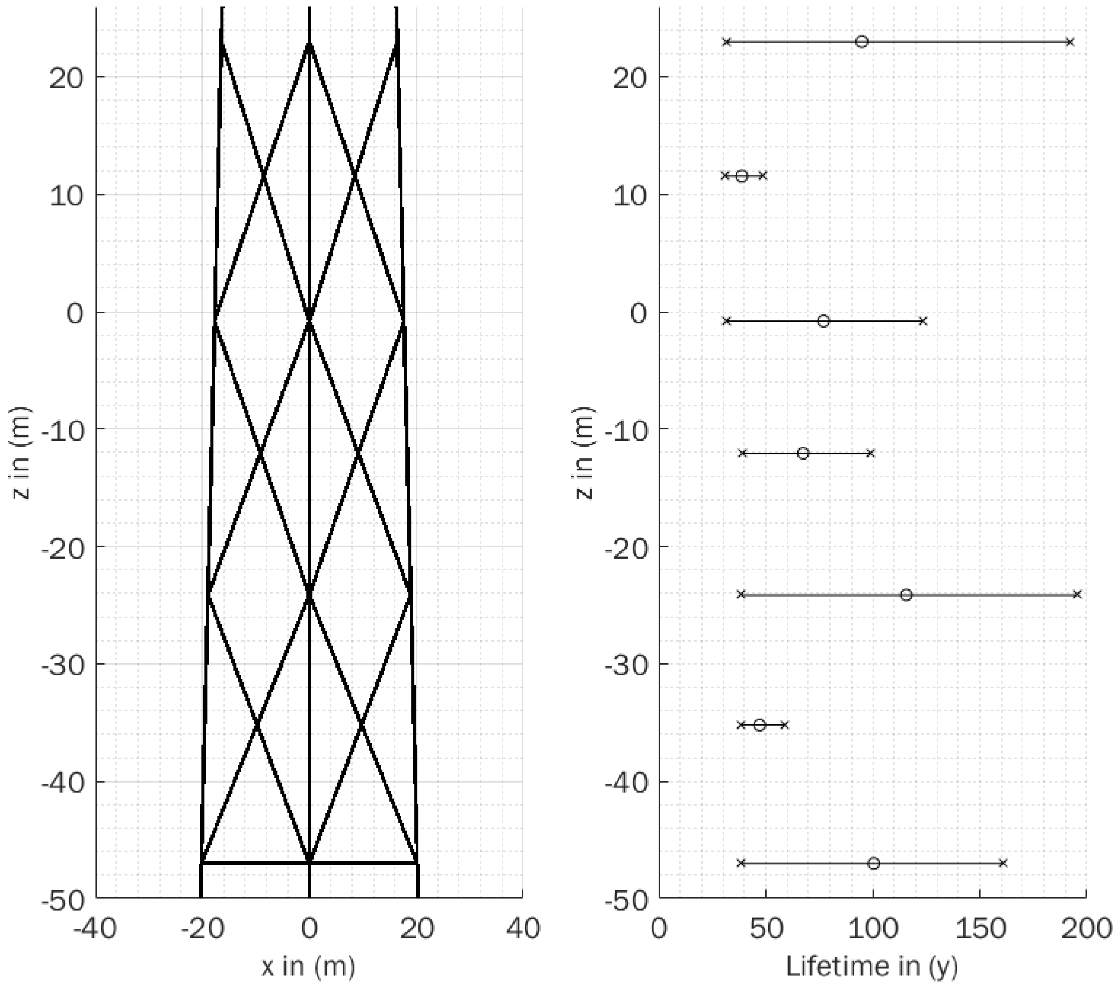

Fig. 10: Hybrid joint lifetimes of ideal jacket for each joint layer. Crosses show the minimum and maximum lifetimes on each layer, circles the corresponding mean lifetime.

A.4. CRAIG-BAMPTON REDUCED EIGENVALUES

SubDyn uses a Component-Mode Synthesis to reduce the number of degrees of freedom. For the calculation of the hybrid jacket, the number of retained modes has been set to a value of 8. The corresponding eigen frequencies is shown in the following table (linearized in zero-deflection operation point):

Mode number	Eigen frequency in Hz
1	4.321
2	5.156
3	5.180
4	5.354
5	5.848
6	5.876
7	6.131
8	6.163

A.5. SUPERELEMENT OF FOUNDATION

Equivalent mass matrix at the TP reference point (obtained by Guyan reduction, linearized in zero-deflection operation point):

	Deflection x	Deflection y	Deflection z	Rotation x	Rotation y	Rotation z
Deflection x	0.390E06	0.542E03	−0.182E03	0.177E05	−0.166E07	0.178E05
Deflection y	0.542E03	0.390E06	0.731E03	0.166E07	−0.451E04	0.351E05
Deflection z	−0.182E03	0.730E03	0.492E06	0.378E04	−0.318E05	−0.286E05
Rotation x	0.177E05	0.166E07	0.379E04	0.648E08	−0.153E05	0.131E06
Rotation y	−0.166E07	−0.451E04	−0.318E05	−0.154E05	0.651E08	−0.205E06
Rotation z	0.180E05	0.351E05	−0.286E05	0.131E06	−0.205E06	0.688E08

Equivalent stiffness matrix at the TP reference point (obtained by Guyan reduction, linearized in zero-deflection operation point):

	Deflection x	Deflection y	Deflection z	Rotation x	Rotation y	Rotation z
Deflection x	0.400E09	0.100E07	0.357E06	0.493E08	−0.118E11	0.382E08
Deflection y	0.100E07	0.400E09	0.256E06	0.118E11	−0.150E08	0.368E08
Deflection z	0.359E06	0.250E06	0.223E10	−0.181E07	−0.282E08	−0.649E08
Rotation x	0.493E08	0.118E11	−0.177E07	0.707E12	−0.921E09	0.104E10
Rotation y	−0.118E11	−0.150E08	−0.282E08	−0.921E09	0.708E12	−0.136E10
Rotation z	0.382E08	0.368E08	−0.648E08	0.104E10	−0.136E10	0.255E12

A.6. SUBDYN INPUT FILE FOR HYBRID-TYPE JACKET

The code of the SubDyn input file of the hybrid-type jacket is given below. The input file can be used with SubDyn version v.1.02 and newer. However, for the calculation a modified version of FAST has been used in order to incorporate the effects of soil-structure interaction, see [15].

```
----------- INNWIND.EU 10MW HYBRID-TYPE JACKET INPUT FILE FOR SUBDYN -----------
--------------------------------------------------------------------------------
-------------------------- SIMULATION CONTROL ----------------------------------
False Echo
"DEFAULT" SDdeltaT
3 IntMethod
True SttcSolve
-------------------- FEA and CRAIG-BAMPTON PARAMETERS --------------------------
3 FEMMod
3 NDiv
True CBMod
8 Nmodes
1.000000 JDampings
--- STRUCTURE JOINTS: joints connect structure members (~Hydrodyn Input File) --
48 NJoints
JointID JointXss JointYss JointZss -Coordinates of Member joints in SS-Coordinate
System
(-) (m) (m) (m)
1 -0.000000 -20.340000 -50.001000
2 20.340000 0.000000 -50.001000
3 0.000000 20.340000 -50.001000
4 -20.340000 -0.000000 -50.001000
5 -0.000000 -20.179400 -47.000000
6 20.179400 0.000000 -47.000000
7 0.000000 20.179400 -47.000000
8 -20.179400 -0.000000 -47.000000
9 9.774100 -9.774100 -35.205800
10 9.774100 9.774100 -35.205800
11 -9.774100 9.774100 -35.205800
12 -9.774100 -9.774100 -35.205800
13 -0.000000 -19.548100 -35.205800
14 19.548100 0.000000 -35.205800
15 0.000000 19.548100 -35.205800
16 -19.548100 -0.000000 -35.205800
17 0.000000 -18.955100 -24.127200
18 18.955100 -0.000000 -24.127200
19 -0.000000 18.955100 -24.127200
20 -18.955100 0.000000 -24.127200
21 9.154700 -9.154700 -12.064700
22 9.154700 9.154700 -12.064700
23 -9.154700 9.154700 -12.064700
24 -9.154700 -9.154700 -12.064700
25 -0.000000 -18.309500 -12.064700
26 18.309500 0.000000 -12.064700
27 0.000000 18.309500 -12.064700
28 -18.309500 -0.000000 -12.064700
29 0.000000 -17.706300 -0.796900
30 17.706300 -0.000000 -0.796900
31 -0.000000 17.706300 -0.796900
32 -17.706300 0.000000 -0.796900
33 8.522800 -8.522800 11.545500
34 8.522800 8.522800 11.545500
35 -8.522800 8.522800 11.545500
36 -8.522800 -8.522800 11.545500
37 -0.000000 -17.045700 11.545500
38 17.045700 0.000000 11.545500
39 0.000000 17.045700 11.545500
40 -17.045700 -0.000000 11.545500
41 -0.000000 -16.432600 23.000000
42 16.432600 0.000000 23.000000
43 0.000000 16.432600 23.000000
```

```
44 -16.432600 -0.000000 23.000000
45 -0.000000 -16.272000 26.000000
46 16.272000 0.000000 26.000000
47 0.000000 16.272000 26.000000
48 -16.272000 -0.000000 26.000000

------ BASE REACTION JOINTS: 1/0 for Locked/Free DOF @ each Reaction Node ------
4 NReact
RJointID RctTDXss RctTDYss RctTDZss RctRDXss RctRDYss RctRDZss - Global Coordinate
System
(-)       (flag)      (flag)      (flag)      (flag)      (flag)      (flag)
1 1 1 1 1 1 1
2 1 1 1 1 1 1
3 1 1 1 1 1 1
4 1 1 1 1 1 1
------------ INTERFACE JOINTS: 1/0 for Locked (to the TP)/Free DOF -------------
4 NInterf
IJointID ItfTDXss ItfTDYss ItfTDZss ItfRDXss ItfRDYss ItfRDZss - Global Coordinate
System
(-)       (flag)      (flag)      (flag)      (flag)      (flag)      (flag)
45 1 1 1 1 1 1
46 1 1 1 1 1 1
47 1 1 1 1 1 1
48 1 1 1 1 1 1
---------------------------------- MEMBERS -------------------------------------
84 NMembers
MemberID MJointID1 MJointID2 MPropSetID1 MPropSetID2 COSMID
(-)         (-)         (-)          (-)           (-)           (-)
1 1 5 1 1
2 2 6 1 1
3 3 7 1 1
4 4 8 1 1
5 5 13 1 1
6 9 5 8 8
7 9 17 5 5
8 9 6 5 5
9 9 18 8 8
10 13 17 2 2
11 6 14 1 1
12 10 6 8 8
13 10 18 5 5
14 10 7 5 5
15 10 19 8 8
16 14 18 2 2
17 7 15 1 1
18 11 7 8 8
19 11 19 5 5
20 11 8 5 5
21 11 20 8 8
22 15 19 2 2
23 8 16 1 1
24 12 8 8 8
25 12 20 5 5
26 12 5 5 5
27 12 17 5 5
28 16 20 2 2
29 17 25 2 2
30 21 17 9 9
31 21 29 6 6
32 21 18 6 6
33 21 30 9 9
34 25 29 3 3
35 18 26 2 2
36 22 18 9 9
37 22 30 6 6
38 22 19 6 6
39 22 31 9 9
40 26 30 3 3
41 19 27 2 2
42 23 19 9 9
```

```
43 23 31 6 6
44 23 20 6 6
45 23 32 9 9
46 27 31 3 3
47 20 28 2 2
48 24 20 9 9
49 24 32 6 6
50 24 17 6 6
51 24 29 6 6
52 28 32 3 3
53 29 37 3 3
54 33 29 10 10
55 33 41 7 7
56 33 30 7 7
57 33 42 10 10
58 37 41 4 4
59 30 38 3 3
60 34 30 10 10
61 34 42 7 7
62 34 31 7 7
63 34 43 10 10
64 38 42 4 4
65 31 39 3 3
66 35 31 10 10
67 35 43 7 7
68 35 32 7 7
69 35 44 10 10
70 39 43 4 4
71 32 40 3 3
72 36 32 10 10
73 36 44 7 7
74 36 29 7 7
75 36 41 7 7
76 40 44 4 4
77 41 45 4 4
78 42 46 4 4
79 43 47 4 4
80 44 48 4 4
81 5 6 5 5
82 6 7 5 5
83 7 8 5 5
84 8 5 5 5
-------- MEMBER X-SECTION PROPERTY data 1/2 [circular-tubular elements] --------
10 NPropSets
YoungE ShearG MatDens XsecD XsecT
PropSetID (N/m2) (N/m2) (kg/m3) (m) (m)
1 2.100000e+11 8.077000e+10 7.850000e+03 1.480000e+00 4.440000e-02
2 2.100000e+11 8.077000e+10 7.850000e+03 1.480000e+00 4.290000e-02
3 2.100000e+11 8.077000e+10 7.850000e+03 1.480000e+00 4.150000e-02
4 2.100000e+11 8.077000e+10 7.850000e+03 1.480000e+00 4.020000e-02
5 2.100000e+11 8.077000e+10 3.965000e+03 1.065600e+00 9.240000e-02
6 2.100000e+11 8.077000e+10 3.965000e+03 1.095200e+00 9.270000e-02
7 2.100000e+11 8.077000e+10 3.965000e+03 1.124800e+00 9.290000e-02
8 2.100000e+11 8.077000e+10 3.965000e+03 9.590000e-01 9.240000e-02
9 2.100000e+11 8.077000e+10 3.965000e+03 9.857000e-01 9.270000e-02
10 2.100000e+11 8.077000e+10 3.965000e+03 1.012300e+00 9.290000e-02
------------- MEMBER X-SECTION PROPERTY data 2/2 [other elements] --------------
0 NXPropSets
YoungE ShearG MatDens XsecA XsecAsx XsecAsy XsecJxx XsecJyy XsecJ0
PropSetID (N/m2) (N/m2) (kg/m3) (m2) (m2) (m2) (m4) (m4) (m4)
---------------------- MEMBER COSINE MATRICES COSM(i,j) ------------------------
0 NCOSMs
COSMID COSM11 COSM12 COSM13 COSM21 COSM22 COSM23 COSM31 COSM32 COSM33
(-)       (-)       (-)       (-)       (-)       (-)       (-)       (-)       (-)
(-)
--------------------- JOINT ADDITIONAL CONCENTRATED MASSES ---------------------
0 NCmass
CMJointID JMass JMXX JMYY JMZZ
(kg) (kg*m2) (kg*m2) (kg*m2)
```

```
-------------------------- OUTPUT: SUMMARY & OUTFILE ---------------------------
False SSSum
False OutCOSM
True OutAll
2 OutSwtch
False TabDelim
1 OutDec
"ES11.4e2" OutFmt
"A11" OutSFmt
------------------------------ MEMBER OUTPUT LIST ------------------------------
0 NMOutputs
MemberID NOutCnt NodeCnt
(-) (-) (-)
------ SSOutList
"-ReactFXss, -ReactFYss, -ReactMXss, -ReactMYss, -ReactMZss, -ReactFZss"
END
```